



# Inversion of an Effective Seismic Force at a Domain Reduction Method (DRM) Boundary and Reconstruction of Wave Responses inside the DRM Boundary

Bruno P. Guidio and Chanseok Jeong

*School of Engineering and Technology, Central Michigan University  
Mount Pleasant, MI 48859, USA  
peruq1b@cmich.edu, jeong1c@cmich.edu (corresponding author)*

**Abstract.** A new inverse modeling is presented for reconstructing an SH wave input motion (i.e., its corresponding effective seismic force vector) in a 2D domain that is truncated by a wave-absorbing boundary condition (WABC). The domain reduction method (DRM) is utilized to model seismic input motions coming from the outside domain of the WABC. The partial differential equation (PDE)-constrained optimization method aims at reconstructing a targeted effective seismic force vector, corresponding to targeted incident wavefields, at the DRM boundary. The presented method includes the discretize-then-optimize (DTO) approach, the finite element method (FEM), which is used for solving state and adjoint problems, and the conjugate-gradient scheme, determining the desired search path throughout a minimization process. The numerical results show that an effective force vector at a DRM boundary is accurately reconstructed when a regularization, aimed at suppressing wave energy in an exterior domain outside a DRM boundary, is utilized in conjunction with a typical misfit functional. By using such a regularization term, the presented algorithm can minimize the kinetic energy associated with scattered wave responses outside the DRM boundary and, eventually, improve the inversion performance. It is also shown that our inverse modeling can accurately reconstruct the wave responses within a domain inside the DRM boundary.

**Keywords:** Domain reduction method, PDE-constrained optimization, Adjoint method, Seismic-input motion inversion, Wave-suppressing regularization.

## 1 Introduction

There is a need to estimate complex seismic input motions in a near-surface domain, without considering a seismic source at a hypocenter, from limited (i.e., sparse in space) seismic measurement data. Based on such estimated seismic inputs, engineers can appropriately investigate the effect of an earthquake on built environments, including subsurface systems (soil, foundations, and underground structures). To date, there have been two dominant, conventional methods for the identification of incident seismic waves that hit a near-surface domain: one is deconvolution in a one-dimensional (1D) setting [1–3] and the other is the inversion of a seismic source profile at a fault in a very large (e.g., hundreds of kilometers long) regional-scale domain [4]. This work presents an alternative to these traditional methods, a new PDE-constrained numerical inversion solver, which is able to identify arbitrary, incoherent incoming seismic waves and reconstruct corresponding wave responses in a truncated multi-dimensional domain by using sparsely measured ground motion.

The inverse problems related with elastodynamic wave motions have improved thanks to PDE-constrained optimization, and the kinds of the associated applications have been extended from material evaluation to dynamic-input identification or optimization. For instance, the PDE-constrained optimization method has been used in the geotechnical site material characterization. [5–9]. To investigate the feasibility to identify arbitrary, incoherent incoming seismic waves in a truncated domain by using the PDE-constrained optimization framework, Jeong and Seylabi [10] and Guidio and Jeong [11] studied a full-waveform source-inversion method to identify an incoming seismic wave in a 1D semi-infinite solid and a 2D bounded domain, respectively. Guidio et al. [12] presented a numerical method that can reconstruct both spatial and temporal distributions of complex, incoherent seismic incident wavefields, modeled as traction on WABC, propagating into a 2D truncated domain of anti-plane shear wave

motion without using any regularization. Guidio and Jeong [13] also discussed a new method for reconstructing an effective force vector at a domain reduction method (DRM) layer and estimating the shear wave motions in an interior domain surrounded by DRM layer. They showed that their numerical method can properly reconstruct the ground motions in the interior domain, but the effective force is not well estimated because their optimizer was not informed of any requirement on the amplitude of the waves resulted from an estimated force vector in an exterior domain.

Continuing the works mentioned before, the presented study considers the DRM and adds a regularization term in the objective functional in order to minimize the wave field in the exterior domain while improve the reconstruction of the targeted effective force vector and its corresponding ground motions.

## 2 Problem definition

The presented method is aimed at (i) identifying an effective seismic force on DRM layer as an incident seismic motion that allows its corresponding wave responses to match the measured motions at sensor locations on the ground surface and (ii) consequently reconstructing wave responses in an interior domain surrounded by the DRM layer. In particular, we impose regularization such that the wave responses in an exterior domain outside the DRM layer due to the estimated force vector are minimized. This work considers a two-dimensional heterogeneous domain of anti-plane shear wave motions as shown in Fig. 1.

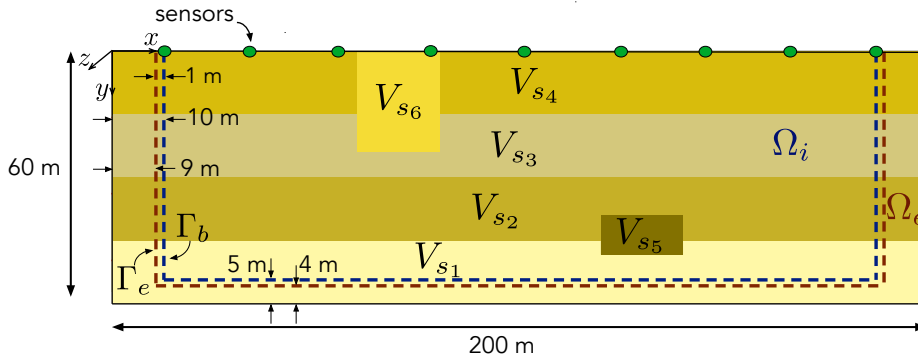


Figure 1. Problem configuration: a DRM-ABC-truncated domain used for an inversion solver.

### 2.1 Governing wave physics

The strong form of the governing differential equation for the shear wave propagation in the domain  $\Omega$  is:

$$\nabla \cdot (G \nabla u) - \rho \frac{\partial^2 u}{\partial t^2} = 0, \quad (1)$$

where  $u = u(x, y, t)$  denotes the displacement field of wave motions in the  $z$ -plane, which is perpendicular to the direction that the wave is moving;  $x$  and  $y$  denote horizontal and vertical coordinates;  $G(x, y)$  and  $\rho(x, y)$  denote the shear modulus and the mass density of the solid.

The traction-free condition is presented on the top surface, while the absorbing boundary conditions are presented on the left, bottom, and right boundaries. The zero initial-value conditions are presented as the system is initially at rest.

Please note that the information on a targeted incident wave motion is not included in this strong form. They will be included in the global force vector per the DRM theory of a discrete form. By using the finite element method, the strong form turns to the following semi-discrete equation:

$$\mathbf{M}\ddot{\mathbf{u}}(t) + \mathbf{C}\dot{\mathbf{u}}(t) + \mathbf{K}\mathbf{u}(t) = \mathbf{F}(t), \quad (2)$$

where  $\mathbf{u}(t)$ ,  $\dot{\mathbf{u}}(t)$ , and  $\ddot{\mathbf{u}}(t)$  denote the displacement, velocity, and acceleration vectors of the state problem at time

$t$ , respectively.  $\mathbf{M}$ ,  $\mathbf{C}$ , and  $\mathbf{K}$  denote the global mass, damping, and stiffness matrices, respectively, while  $\mathbf{F}$  is the global force vector.

## 2.2 Domain reduction method

In Bielak's DRM formulation (Bielak et al., 2003; Yoshimura et al., 2003), the semi-infinite solid is subdivided into three different parts: the interior domain  $\Omega_i$ , an interface  $\Gamma_b$ , and the exterior domain  $\Omega_e$ , as shown in Fig. 1. Besides, the subscripts  $i$ ,  $b$ , and  $e$  are used to denote the nodes on the interior domain of interest, interface, and exterior domain, respectively. The nodes on  $\Gamma_b$ , and their neighboring exterior nodes, localized at the fictitious boundary  $\Gamma_e$ , form the DRM layer. Per the DRM theory, a targeted effective seismic force vector  $\mathbf{F}^{\text{eff}}$ , obtained from free-field ground motions, is applied on all the nodes on the DRM layer in order to consistently model incident seismic waves impinging the domain. Bielak's DRM formulation shows how to use the free-field displacements and acceleration,  $\mathbf{u}^0$  and  $\ddot{\mathbf{u}}^0$ , respectively, at nodes of the DRM layer to determine the effective seismic force vector  $\mathbf{F}^{\text{eff}}$ .

## 2.3 Discrete state problem

The time-dependent semi-discrete equation is solved by considering the initial-value conditions and applying the implicit Newmark time integration. Then, the state problem is formed in the compact form,  $\mathbf{Q}\hat{\mathbf{u}} = \hat{\mathbf{F}}$ , where matrix  $\mathbf{Q}$ , solution vector  $\hat{\mathbf{u}}$ , and global force vector  $\hat{\mathbf{F}}$ , are all defined as shown in the authors' previous work [12].

## 3 Inverse modeling

Under this inversion method, we determine the control parameters as  $P_{b_{kj}}$  and  $P_{e_{kj}}$ . They are components of  $\hat{\mathbf{F}}_{\text{estm}}$  corresponding to  $\gamma_{b_k}$  and  $\gamma_{e_k}$ , respectively, and  $t_j$ :  $\gamma_{b_k}$  is the  $k$ -th discrete node on the DRM boundary  $\Gamma_b$ , and  $\gamma_{e_k}$  is the  $k$ -th discrete node on  $\Gamma_e$ ; and  $t_j$  is the  $j$ -th time step.

### 3.1 Discrete objective and Lagrangian functional

We attempt to determine the values of control parameters that minimize the discrete objective functional, which is defined as:

$$\hat{\mathcal{L}} = \underbrace{0.5(\hat{\mathbf{u}} - \hat{\mathbf{u}}_m)^T \bar{\mathbf{B}} (\hat{\mathbf{u}} - \hat{\mathbf{u}}_m)}_{\text{misfit}} + \underbrace{0.5R \hat{\mathbf{u}}^T \bar{\mathbf{D}} \hat{\mathbf{u}}}_{\text{regularization}}, \quad (3)$$

where  $\hat{\mathbf{u}}$  and  $\hat{\mathbf{u}}_m$  are obtained by a set of targeted and estimated control parameters, respectively, and  $\bar{\mathbf{B}}$  is defined as  $\Delta t \mathbf{B}$ , where  $\mathbf{B}$  a square matrix, of which components are all 0 except for those of the diagonal, having values of all 1, if they correspond to the degrees of freedom at sensor locations. The regularization coefficient is defined as the constant  $R$ , and  $\bar{\mathbf{D}}$  is defined as  $\Delta t \mathbf{D}$ , where  $\mathbf{D}$  is a square matrix, of which components are all 0 except for those of the diagonal, having values of all 1, if they correspond to the nodes on  $\Omega_e$ .

By imposing state equation onto an objective functional by using the Lagrangian multiplier vector  $\hat{\boldsymbol{\lambda}}$ , we cast the following Lagrangian functional:

$$\hat{\mathcal{A}} = 0.5(\hat{\mathbf{u}} - \hat{\mathbf{u}}_m)^T \bar{\mathbf{B}} (\hat{\mathbf{u}} - \hat{\mathbf{u}}_m) + 0.5R \hat{\mathbf{u}}^T \bar{\mathbf{D}} \hat{\mathbf{u}} - \hat{\boldsymbol{\lambda}}^T (\mathbf{Q}\hat{\mathbf{u}} - \hat{\mathbf{F}}_{\text{estm}}). \quad (4)$$

### 3.2 Optimally conditions

To identify unknown target control parameters, the first-order optimality conditions should be fulfilled. The first condition,  $(\partial \hat{\mathcal{A}} / \partial \hat{\boldsymbol{\lambda}}) = 0$ , will be automatically satisfied when we solve the discrete forward problem.

The second condition,  $(\partial \hat{\mathcal{A}} / \partial \hat{\mathbf{u}}) = 0$ , will be automatically satisfied when the adjoint problem is solved:

$$\frac{\partial \hat{A}}{\partial \hat{\mathbf{u}}} = \underbrace{-\mathbf{Q}^T \hat{\lambda} + \mathbf{B}(\hat{\mathbf{u}} - \hat{\mathbf{u}}_m) + R\mathbf{D}\hat{\mathbf{u}}}_{\text{adjoint equation}} = 0. \quad (5)$$

We solve the adjoint problem by marching backward in time as shown in our previous work [12].

The third condition will be satisfied when we solve the control problem,  $(\partial \hat{A} / \partial \hat{\mathbf{F}}_{\text{estim}}) = \hat{\lambda} = 0$ , which implies that a gradient vector,  $\partial \hat{A} / \partial \hat{\mathbf{F}}_{\text{estim}} = \partial \hat{\mathcal{L}} / \partial \hat{\mathbf{F}}_{\text{estim}}$ , is comprised of the component of the vector  $\hat{\lambda}$  corresponding to the global node numbering and time step of control parameters.

### 3.3 Control parameters updates

By using the semi-analytical evaluated, gradient vector this work iteratively updates the estimated control parameters as follows. First, the conjugate-gradient method determines the best search direction, and an optimal step length is calculated by Newton's method [11]. Then, the gradient-based minimization scheme updates the control parameters by summing the previous control parameters and the product between the search direction and optimal step length. We perform the numerical experiments of the presented inversion method by using our in-house forward and inverse wave solver written in MATLAB.

## 4 Numerical Experiment

In this section, a numerical experiment is considered where the ground motions are induced by a vertically-propagating 1D free-field wave in the domain shown in Fig. 1. Its dimension is  $200 \text{ m} \times 60 \text{ m}$ , and the shear wave speeds are  $V_{s_1} = 300 \text{ m/s}$ ,  $V_{s_2} = 250 \text{ m/s}$ ,  $V_{s_3} = 200 \text{ m/s}$ ,  $V_{s_4} = 150 \text{ m/s}$ ,  $V_{s_5} = 800 \text{ m/s}$ , and  $V_{s_6} = 1000 \text{ m/s}$ . The mass density is  $1500 \text{ kg/m}^3$ , and it is uniform in the entire domain. A Ricker waleter signal of a central frequency of 5 Hz is used as the time signal of the vertically-propagating wave, and sensors are distributed on the top surface with a 5 m spacing of each other.

The example studies the performance of the presented inversion solver for reconstructing  $\hat{\mathbf{F}}^{\text{eff}}$  and the ground motions induced by the 1D incident waves. For appraising the accuracy of the presented inverse modeling, the error norms  $\mathcal{E}$  and  $\mathcal{E}^u$  are calculated to evaluate the inversion performance to reconstruct  $\hat{\mathbf{F}}^{\text{eff}}$  and ground motions in  $\Omega_i$ , respectively.

Figure 2 shows the ground motions induced by targeted effective force and their reconstructed counterparts without and with using the presented regularization. As shown in the second row of Fig. 2, the reconstructed ground motions without using the regularization term in the objective functional have a larger amplitude in  $\Omega_e$  than their targeted counterparts. It is because the minimizer is not provided with any information about the DRM modeling, specifically with respect to the wave responses in  $\Omega_e$ . Consequently, even though the error  $\mathcal{E}^u$  between the targeted and estimated wave responses in  $\Omega_i$  is only 1.40%, Fig. 3 shows that the reconstructed force vector without using the regularization significantly differs from its targeted counterpart ( $\mathcal{E} = 99.03\%$ ).

By utilizing the regularization, the amplitudes of waves in  $\Omega_e$  due to the estimated force vector are minimized (see the last row of Fig. 2). Consequently, the presented inversion solver can better reconstruct the targeted effective force vector, as shown in the last column of Fig. 3. After 10,000 iterations using the regularization, the error  $\mathcal{E}^u$  between the targeted and estimated ground motions in  $\Omega_i$  is 5.47%. Although the error  $\mathcal{E}^u$  increased comparing with the case without regularization, the error  $\mathcal{E}$  between the targeted and reconstructed force vector dropped to 46.91%.

## 5 Conclusions

In this study, we explored a new approach for (i) identifying an effective seismic force on a DRM layer as an incident seismic motion and (ii) reconstructing wave responses in the interior domain in a 2D domain of anti-plane shear wave motions truncated by WABC. In the presented method, the DRM is used to model incident waves into the domain, the gradient-based minimization is utilized to tackle the inverse problem, and the DTO approach is employed to solve the adjoint problem. It was shown that the wave responses in an interior domain surrounded by a DRM layer can be reconstructed by using the presented method. Furthermore, the regularization term in the objective functional helps our optimizer minimize the wave responses in the exterior domain and consequently better reconstruct the targeted effective force.

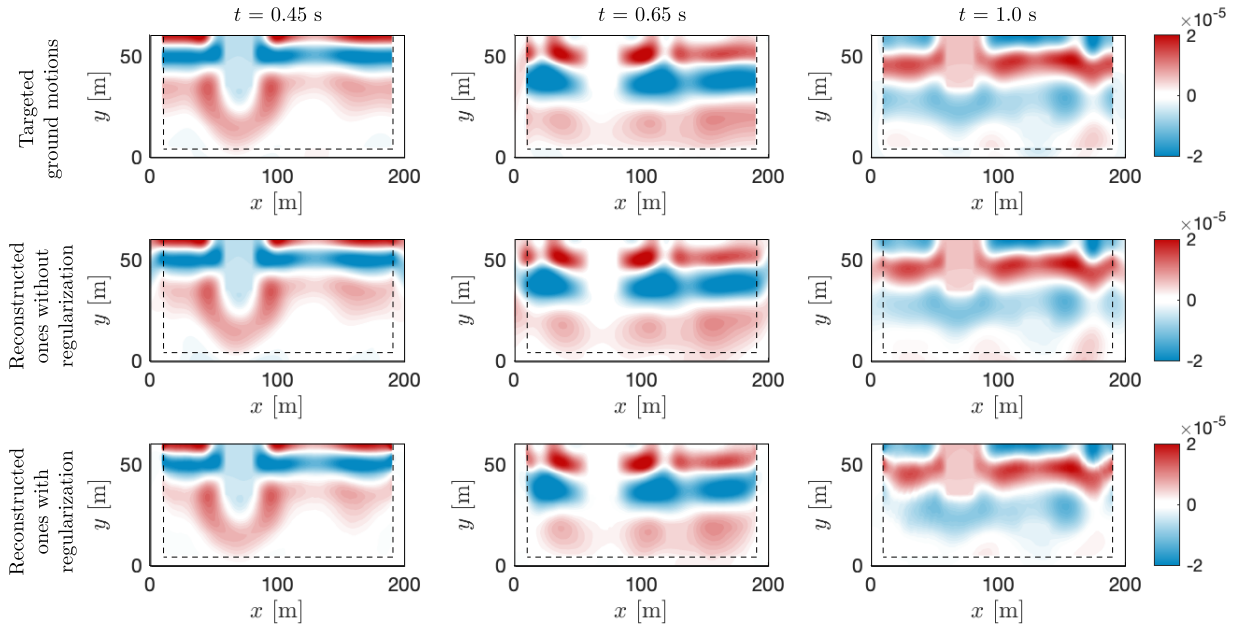


Figure 2. Wave responses in the domain induced by (*top row*) the targeted effective force, (*middle row*) its reconstructed counterpart without using the regularization, and (*bottom row*) its reconstructed counterpart using the regularization. The dashed line indicates the DRM boundary  $\Gamma_b$ .

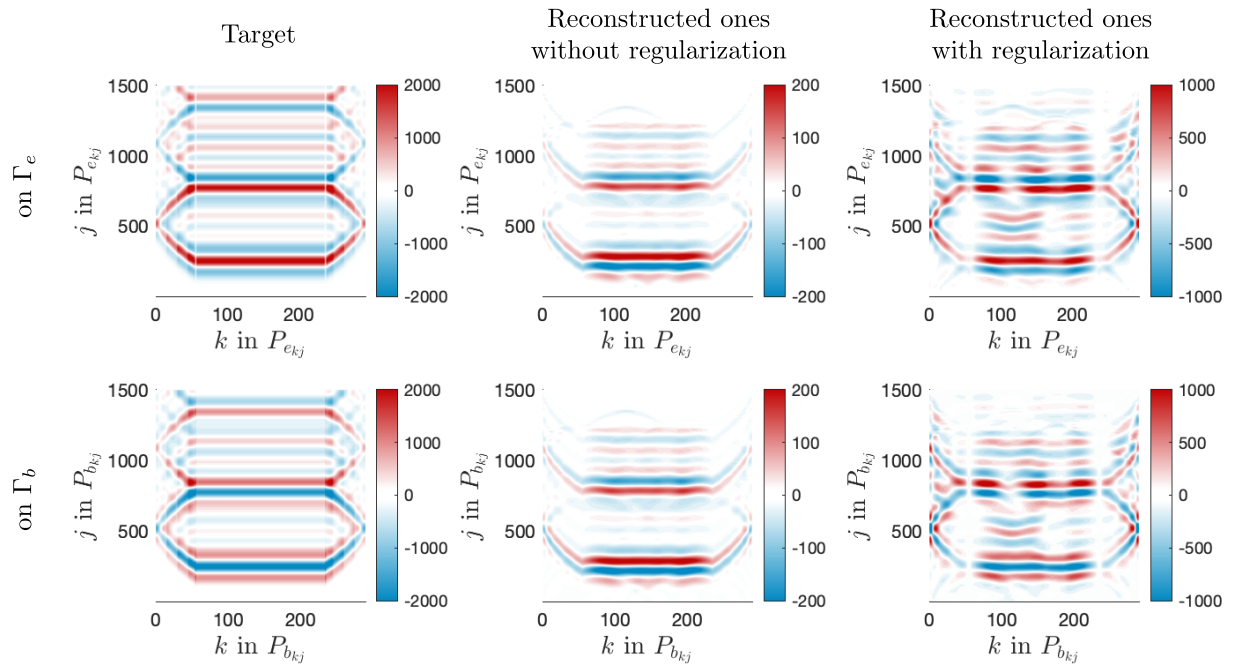


Figure 3. Targeted effective seismic force, its reconstructed counterpart without using the regularization, and its reconstructed counterpart using the regularization, on  $\Gamma_e$  and  $\Gamma_b$ .

**Acknowledgements.** This material is based upon work supported by the National Science Foundation under Award CMMI-1855406 and CMMI-2044887. Any opinions, findings, and conclusions or recommendations expressed in this material are those of the authors and do not necessarily reflect the views of the National Science Foundation. The authors are also grateful for the support by the Faculty Research and Creative Endeavors (FRCE) Research Grant 48058 at Central Michigan University.

**Authorship statement.** The authors hereby confirm that they are the sole liable persons responsible for the authorship of this work, and that all material that has been herein included as part of the present paper is either the property (and authorship) of the authors, or has the permission of the owners to be included here.

## References

- [1] L. Mejia and E. Dawson. Earthquake deconvolution for flac. In *4th International FLAC symposium on numerical modeling in geomechanics*, pp. 04–10, 2006.
- [2] M. K. Poul and A. Zerva. Efficient time-domain deconvolution of seismic ground motions using the equivalent-linear method for soil-structure interaction analyses. *Soil Dynamics and Earthquake Engineering*, vol. 112, pp. 138 – 151, 2018a.
- [3] M. K. Poul and A. Zerva. Nonlinear dynamic response of concrete gravity dams considering the deconvolution process. *Soil Dynamics and Earthquake Engineering*, vol. 109, pp. 324 – 338, 2018b.
- [4] V. Akcelik, G. Biros, and O. Ghattas. Parallel multiscale Gauss-Newton-Krylov methods for inverse wave propagation. In *Supercomputing, ACM/IEEE 2002 Conference*, pp. 41–41. IEEE, 2002.
- [5] C. Jeong, S.-W. Na, and L. F. Kallivokas. Near-surface localization and shape identification of a scatterer embedded in a halfplane using scalar waves. *Journal of Computational Acoustics*, vol. 17, n. 03, pp. 277–308, 2009.
- [6] J. W. Kang and L. F. Kallivokas. The inverse medium problem in 1D PML-truncated heterogeneous semi-infinite domains. *Inverse Problems in Science and Engineering*, vol. 18, n. 6, pp. 759–786, 2010.
- [7] K. T. Tran and M. McVay. Site characterization using Gauss-Newton inversion of 2-D full seismic waveform in the time domain. *Soil Dynamics and Earthquake Engineering*, vol. 43, pp. 16–24, 2012.
- [8] A. Fathi, L. F. Kallivokas, and B. Poursartip. Full-waveform inversion in three-dimensional PML-truncated elastic media. *Computer Methods in Applied Mechanics and Engineering*, vol. 296, pp. 39–72, 2015.
- [9] A. Fathi, B. Poursartip, K. H. Stokoe II, and L. F. Kallivokas. Three-dimensional P-and S-wave velocity profiling of geotechnical sites using full-waveform inversion driven by field data. *Soil Dynamics and Earthquake Engineering*, vol. 87, pp. 63–81, 2016.
- [10] C. Jeong and E. E. Seylabi. Seismic input motion identification in a heterogeneous halfspace. *Journal of Engineering Mechanics*, vol. 144, n. 8, pp. 04018070, 2018.
- [11] B. P. Guidio and C. Jeong. Full-waveform inversion of incoherent dynamic traction in a bounded 2D domain of scalar wave motions. *Journal of Engineering Mechanics*, vol. 147, n. 4, pp. 04021010, 2021a.
- [12] B. Guidio, B. Jeremic, L. P. Guidio, and C. Jeong. Passive-seismic inversion of SH-wave input motions in a domain truncated by wave absorbing boundary condition. Under Review, 2021.
- [13] B. Guidio and C. Jeong. Reconstruction of Seismic-wave responses in a domain surrounded by a domain reduction method layer. Under Review, 2021b.